JOURNAL OF AGRICULTURAL AND FOOD CHEMISTRY

Article

pubs.acs.org/JAFC

α-Glucosidase Inhibitors via Green Pathway: Biotransformation for Bicoumarins Catalyzed by *Momordica charantia* Peroxidase

Xiao-Jun Hu, Xiao-Bing Wang, and Ling-Yi Kong*

State Key Laboratory of Natural Medicines, Department of Natural Medicinal Chemistry, China Pharmaceutical University, 24 Tong Jia Xiang, Nanjing 210009, People's Republic of China

Supporting Information

ABSTRACT: Peroxidase extracted from *Momordica charantia* catalyzed the H_2O_2-dependent oxidative coupling of 7-hydroxy-4-methylcoumarin to form four new dimers (**1**−**4**) and two known ones (**5**, **6**). The structures, including the absolute configurations of axially chiral compounds, were unambiguously characterized by NMR spectroscopy, online HPLC-CD, and a variety of computational methods. Bioactive experiments demonstrated that compounds **1** and **2** had significant inhibitory effects on yeast α-glucosidase, much better than the controls. Noncompetitive binding mode was found by the graphical analysis of steady-state inhibition data. The mechanism of enzymatic inhibition confirmed in some depth that the inhibitors altered the secondary structure of α-glucosidase by decreasing the α-helix and increasing the β-sheet content. In summary, bicoumarins **1** and **2** might be exploited as the lead compounds for further research of antidiabetic agents, and this research provided a "green" method to synthesize compounds with the chiral biaryl axis generally calling for multistep reactions in organic chemistry.

KEYWORDS: *Momordica charantia peroxidase, 7-hydroxy-4-methylcoumarin, biotransformation, bicoumarin, α-glucosidase inhibitor*

INTRODUCTION

Diabetes mellitus, as a health-threatening concomitant disease all over the world, is a chronic metabolic disease associated with disorders of carbohydrate metabolism and characterized by hyperglycemia.[1−4] The control of postprandial blood glucose excursions has come to the fore of the treatment of diabetes.[5] One of the therapeutic approaches to reduce postprandial hyperglycemia is to retard digestion and absorption of dietary carbohydrates by inhibiting digesting enzymes, such as α-glucosidase and α-amylase, in the digestive organs.[6] α-Glucosidase inhibitors, the effective therapeutic agents for type II diabetes and obesity, have a widespread clinical use for managing blood glucose levels. However, most of the developed α-glucosidase inhibitors are sugar mimics requiring multiple steps from carbohydrates and noncarbohydrates,[7] including 1-deoxynojirimycin,[8] valienamine,[9] and acarbose.[10] Consequently, it is necessary to utilize a simple and economical synthetic method to obtain α-glucosidase inhibitors.

Modern biotransformation, which is regarded as a highly efficient and environment-friendly technology, is scoring new achievements in the pharmaceutical field.[11−14] Plant peroxidase is found to play a key role in biotransformation by catalyzing oxidoreduction between hydrogen peroxide and various reductants.[15−17] Acting as an important peroxidase in plants, *Momordica charantia* peroxidase (MCP), exclusively obtained from the fresh fruits of *M. charantia*, has proven to be a useful and versatile catalyst with favorable enzyme pH stability (pH 3.8−8.0) and thermostability (20−45 °C).[18−20] According to current wisdom, the biotransformation research of natural products by MCP focused on the phenylpropanoids[18,19] and stilbenes.[20,21] Of these above reports, oligomers were acquired, and many of them exhibited apparent biological activities.

Although there has been no related biotransformation report on members of the coumarin family, coumarins and their derivatives seem to be good substrates for MCP, with a wide spectrum of biological activities, such as anticancer,[22] antibacterial,[23] anti-HIV,[24] and anti-inflammatory.[25] In addition, coumarin monomers such as 7-hydroxy-4-methylcoumarin have also displayed potent α-glucosidase inhibitory activity *in vitro*, resulting in lowering high blood sugar.[26,27] These facts and strong catalytic ability of MCP prompted us to study the enzymatic biotransformation of 7-hydroxy-4-methylcoumarin by MCP and α-glucosidase inhibition of the oligomeric products. Herein, we reported the biotransformation course, the isolation and structural identification of the products, and the absolute configurations of axially chiral compounds. Electronic circular dichroism (ECD) spectra and the barriers of rotation around the biaryl bond were calculated by density functional theory (DFT). We also evaluated the yeast α-glucosidase inhibitory potential of the bicoumarins for the first time and provided an in-depth analysis of the kinetics and the mechanism of enzymatic inhibitors.

MATERIALS AND METHODS

General Experimental Procedures. Optical rotations were measured with a Jasco P-1020 polarimeter (Jasco, Tokyo, Japan). CD spectra were obtained on a Jasco 810 spectropolarimeter (Jasco, Tokyo, Japan). Ultraviolet (UV) spectra were recorded on a UV-2450 UV/vis spectrophotometer (Shimadzu, Tokyo, Japan). IR (KBr disks) spectra were recorded on a Bruker Tensor 27 spectrometer (Bruker, Karlsruhe, Germany). ^{1}H and ^{13}C NMR, HSQC, HMBC, and NOESY spectra were performed with a Bruker AV-500 NMR (500 and 125 MHz for ^{1}H and ^{13}C NMR, respectively) instrument (Bruker, Karlsruhe, Germany) in MeOH-d_4 or DMSO-d_6, with tetramethylsi-

Received: October 14, 2012
Revised: January 26, 2013
Accepted: January 29, 2013
Published: January 29, 2013

ACS Publications © 2013 American Chemical Society

dx.doi.org/10.1021/jf304384b | J. Agric. Food Chem. 2013, 61, 1501−1508

Table 1. ^{1}H NMR (500 MHz) and ^{13}C NMR (125 MHz) Data of 1−4

	1[a]		2[b]		3[b]		4[b]	
no.	δ_H	δ_C	δ_H	δ_C	δ_H	δ_C	δ_H	δ_C
2		162.9		160.0		160.5		157.3
3		114.0		118.5	6.05 (s)	108.6		132.6
4		154.2		149.5		154.3		142.9
5	7.69 (d, 7.5)	127.4	7.63 (d, 8.5)	126.8	7.56 (d, 9.0)	124.7	7.62 (d, 8.5)	127.5
6	6.86 (dd, 2.0, 7.5)	114.7	6.81 (dd, 2.0, 8.5)	113.1	6.89 (d, 9.0)	114.8	6.84 (dd, 2.5, 8.5)	114.3
7		163.3		161.5		163.8		160.8
8	6.78 (d, 2.0)	103.5	6.71 (d, 2.0)	101.9		114.4	6.73 (d, 2.5)	102.8
9		156.3		154.0		152.6		153.3
10		111.4		112.0		111.8		112.3
2′		163.9		160.4		160.7		162.4
3′	6.11 (s)	111.2	6.08 (s)	109.5	6.06 (s)	108.9	6.27 (s)	112.3
4′		156.5		153.5		154.0		154.1
5′	7.71 (d, 7.5)	128.1	7.47 (s)	128.0	7.61 (s)	128.9	7.73 (d, 8.5)	127.5
6′	6.97 (d, 7.5)	114.5		120.5		119.9	7.08 (dd, 2.5, 8.5)	112.8
7′		161.5		161.0		164.0		160.2
8′		115.5	6.76 (s)	102.4	6.75 (s)	103.4	7.05 (d, 2.5)	102.9
9′		154.6		154.6		153.7		154.9
10′		114.3		111.9		109.1		115.3
4-Me	2.22 (s)	16.6	2.15 (s)	16.1	2.40 (s)	18.4	2.29 (s)	12.0
4′-Me	2.48 (s)	18.9	2.33 (s)	18.0	2.33 (s)	18.1	2.41 (s)	18.6

[a]Recorded in CD_3OD. [b]Recorded in DMSO-d_6.

lane (TMS) as the internal standard. Electrospray ionization (ESI) and high-resolution (HR) ESI mass spectral data were acquired on an Agilent 1100 series LC/MSD ion trap mass spectrometer and a G1969A TOF-MS instrument (Agilent, Santa Clara, CA), respectively. Preparative HPLC was carried out using an Agilent 1200 Series with a Shim-pak RP-C18 column (20 mm i.d. × 200 mm) (Shimadzu, Japan) and a 1200 Series multiple-wavelength detector at 210 and 330 nm. Chiralpak AD-H columns (0.46 i.d. × 25 cm) were purchased from Daicel Chemical Ltd. (Shanghai, China). The HPLC-CD coupling system consisted of a Jasco PU-2089 intelligent pump with a column oven (Jasco CO-206Plus), a Rheodyne 7725 injector with a 20 μL sample loop, and a Jasco CD-2095Plus CD chiral detector (Hg−Xe lamp) (Jasco, Tokyo, Japan). α-Glucosidase inhibitory activity was measured spectrophotometrically using a Spectra Max Plus 384 multidetection microplate reader (Molecular Devices, Sunnyvale, CA). α-Glucosidase (EC 3.2.1.20) was purchased from Oriental Yeast Co., Ltd. (Tokyo, Japan). *p*-Nitrophenyl-α-D-glucopyranoside (*p*-NPG), 1-deoxynojirimycin, and genistein were from Sigma (Sigma-Aldrich, St. Louis, MO). Other reagents and solvents used were of analytical grade and were purchased from reliable commercial sources.

Plant Materials. The fresh fruits of *M. charantia*, identified by Prof. Min-jian Qin of China Pharmaceutical University, were purchased in a suburb of Nanjing, China. A voucher specimen (no. 000804) was deposited in the Department of Natural Medicinal Chemistry, China Pharmaceutical University.

Purification of MCP. MCP was purified from the fresh fruits of *M. charantia* to electrophoretic homogeneity by consecutive treatment of ammonium sulfate fractionation, ion exchange chromatography on DEAE-Sepharose FF, affinity chromatography on Con A Sepharose, and gel filtration on Sephadex G-150 as described in our previous report.[18,19] The purified MCP exhibited a specific activity of 7588 EU of peroxidase per mg of protein, which was 45-fold higher than that of the crude extract.

Biotransformation of 7-Hydroxy-4-methylcoumarin in Aqueous Acetone. 7-Hydroxy-4-methylcoumarin (0.66 g) was dissolved in a NaOAc−HOAc buffer (0.1 M, pH 5.0)/acetone solution (70:30 v/v, 180 mL), and peroxidase (4×10^3 U) in NaOAc−HOAc buffer was added at 37 °C. Six aliquots of hydrogen peroxide (0.3%, 15 mL) were added in 40 min intervals. After a total reaction time of 4 h, the reaction mixture was evaporated to dryness under reduced pressure. Ethyl acetate extraction was performed three times; the organic extract was washed with distilled water, dried over anhydrous Na_2SO_4, and vacuum-concentrated to afford a light yellow powder (0.55 g). Incubations of 7-hydroxy-4-methylcoumarin without MCP or H_2O_2 were used as the experimental controls.

Isolation and Identification. The products were subjected to RP-C18 column chromatography (Φ 3.0 × 50, 80 g) eluted with a gradient solvent system of MeOH−H_2O (40:60 to 60:40, v/v) to yield fraction A (63 mg), fraction B (125 mg), and fraction C (32 mg). Fraction A was chromatographed on a Sephadex LH-20 column (Φ 1.5 × 100, 70 g) eluted with MeOH and isolated by preparative (prep)-HPLC (MeOH−0.05% TFA in H_2O, 35:65, v/v) to give **3** (10 mg) and **6** (18 mg). Fraction B was applied to Sephadex LH-20 column chromatography (Φ 1.5 × 100, 70 g) with MeOH and then separated by prep-HPLC (MeOH−0.05% TFA in H_2O, 48:52, v/v) to obtain **1** (27 mg), **2** (32 mg), and **5** (8 mg). Fraction C was subjected to Sephadex LH-20 column chromatography (Φ 1.5 × 100, 70 g) eluted with MeOH and finally purified by prep-HPLC (MeOH−0.05% TFA in H_2O, 56:44, v/v) to afford **4** (6 mg).

Data for compound ***1****:* white, amorphous powder; IR (KBr) ν_{max} 3442, 2925, 2853, 1674, 1612, 1510, 1392, 1165 cm^{-1}; UV λ_{max} (MeOH) 218, 294, 332 nm; ESIMS *m/z* 351 $[M + H]^+$; HRESIMS (positive mode) *m/z* 373.0688 $[M + Na]^+$ (calcd for $C_{20}H_{14}O_6Na$, 373.0683); ^{1}H and ^{13}C NMR data, see Table 1.

Data for compound ***2****:* white, amorphous powder; IR (KBr) ν_{max} 3442, 2920, 2850, 1686, 1620, 1573, 1391, 1153 cm^{-1}; UV λ_{max} (MeOH) 218, 296, 338 nm; ESIMS *m/z* 351 $[M + H]^+$; HRESIMS (positive mode) *m/z* 373.0686 $[M + Na]^+$ (calcd for $C_{20}H_{14}O_6Na$, 373.0683); ^{1}H and ^{13}C NMR data, see Table 1.

Data for compound ***3****:* white, amorphous powder; IR (KBr) ν_{max} 3424, 2924, 2853, 1629, 1384, 1114 cm^{-1}; UV λ_{max} (MeOH) 218, 294, 332 nm; ESIMS *m/z* 373 $[M + Na]^+$; HRESIMS (positive mode) *m/z* 373.0684 $[M + Na]^+$ (calcd for $C_{20}H_{14}O_6Na$, 373.0683); ^{1}H and ^{13}C NMR data, see Table 1.

Data for compound ***4****:* white, amorphous powder; IR (KBr) ν_{max} 3450, 2924, 2853, 1679, 1398, 1141 cm^{-1}; UV λ_{max} (MeOH) 216, 292, 330 nm; ESIMS *m/z* 351 $[M + H]^+$; HRESIMS (positive mode) *m/z* 373.0680 $[M + Na]^+$ (calcd for $C_{20}H_{14}O_6Na$, 373.0683); ^{1}H and ^{13}C NMR data, see Table 1.

Stereoisomer Analysis by Online Chiral HPLC-CD Coupling. Chiral analyses were carried out by using Chiralpak AD-H columns at 35 °C and a detection wavelength of 330 nm. The solvent system (*n*-

hexane−2-propanol−TFA = 70:30:0.1, v/v/v) was used at the rate of 1 mL/min under isocratic conditions. Chromatographic separations were performed using a Jasco PU-2089 intelligent pump with a column oven (Jasco CO-206Plus) and a Jasco CD-2095Plus CD chiral detector (Hg−Xe lamp), simultaneously monitoring the CD and UV signals at one specific wavelength (range 220−420 nm).

Calculation Details. All calculations were performed with the Gaussian 09 program package.[28] The potential energy surface of compound **1** was scanned using the DFT method at the 6-31G+(d,p) level. Full geometry optimizations were performed for compound **1** and the transition state of racemization, and frequency analyses were carried out to identify the nature (minima or transition state) of the optimized geometries. The ECD calculations of compound **1** were performed with the TDDFT method at the B3LYP/6-31G+(d,p) level of theory. The rotatory strengths were summed and energetically weighted following the Boltzmann statistics. Then, the CD curves were simulated by using the following Gaussian function:

$$\Delta\varepsilon(E) = \frac{2}{2.296 \times 10^{-39}} \times \frac{1}{\sqrt{\pi}w} \sum_i \Delta E_{0i} R_{0i} e^{-[2(E-\Delta E_{0i})/w]^2}$$

where w is the bandwidth at $1/e$ peak height and expressed in energy units. ΔE_{0i} and R_{0i} are the excitation energies and rotatory strengths for the transition from 0 to i, respectively.[29]

Yeast α-Glucosidase Inhibitory Activity. The α-glucosidase inhibition was assessed according to the slightly modified method of Tsujii et al.[30] The α-glucosidase (1.0 U/mL) and substrate (1.0 mM *p*-nitrophenyl-α-D-glucopyranoside) were dissolved in 50 mM pH 6.8 sodium phosphate buffer. The inhibitor was preincubated with α-glucosidase at 37 °C for 0.5 h, and then the substrate was added to the reaction mixture. The enzymatic reaction was carried out at 37 °C for 0.5 h. The absorbance at 405 nm was determined using a microplate reader. All samples were analyzed in triplicate with five different concentrations around the IC_{50} values, and the mean values were taken. The inhibition percentage (%) was calculated by the following equation: Inhibition (%) = $[1 - (A_{sample}/A_{control})] \times 100$.

Kinetics of α-Glucosidase Inhibitors. The enzyme−inhibitor reaction was performed according to the method described above in the absence or presence of varying inhibitor concentrations. Inhibition types and K_i values of the inhibitors were determined by the Lineweaver−Burk plot, a linear double-reciprocal plot of the substrate concentration and reaction velocity. The K_i reported was the mean of the K_i values obtained from each of the different inhibitor concentrations.

Secondary Structure Studies. CD was performed to examine the characterization of the secondary structure of α-glucosidase with a J-810 spectropolarimeter in the UV range (190−250 nm), using 1 mm quartz cuvettes. The CD spectra were recorded with 3 times accumulation. The data of the secondary structure obtained from the experiments were dealt with using the professional software Secondary Structure Estimation and GraphPad Prism 5.

RESULTS AND DISCUSSION

Proposed Mechanism of Biotransformation. Compared with experimental controls, the results of HPLC analysis explained that MCP was a H_2O_2-dependent oxidative enzyme, and MCP and H_2O_2 were essential for these biotransformation products (see Figure S1 in the Supporting Information). Catalyzed by MCP, the biotransformation of 7-hydroxy-4-methylcoumarin was the oxidative process of a free-radical mechanism (Figure 2): using H_2O_2 as electron acceptor, 7-hydroxy-4-methylcoumarin was dehydrogenated and reproduced various radicals (**a**−**d**), resulting in self-coupling reactions to form diverse carbon−carbon and carbon−oxygen polymers. Generally, no regio- or stereoselectivity was observed in radical reactions, so the products of biotransformation were racemates.

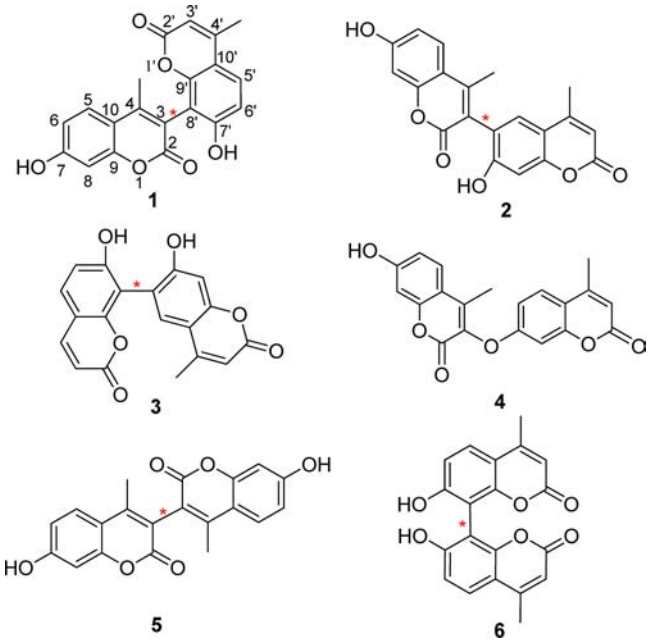

Figure 1. Structures of **1**−**6**.

Structure Identification of Biotransformation Products. Compound **1**, a white, amorphous powder, had a molecular formula of $C_{20}H_{14}O_6$ as established by the HRESIMS ion at m/z 373.0688 $[M + Na]^+$, indicating the formation of a 7-hydroxy-4-methylcoumarin dimer. The IR analysis of **1** indicated the presence of a hydroxyl group (3442 cm^{-1}) and a carbonyl group (1674 cm^{-1}). The ^1H NMR (Table 1) spectrum showed five aromatic proton signals at δ 7.71 (d, J = 7.5 Hz), 7.69 (d, J = 7.5 Hz), 6.97 (d, J = 7.5 Hz), 6.86 (dd, J = 2.0, 7.5 Hz), and 6.78 (d, J = 2.0 Hz), which were assigned to an ABX spin system of one coumarin moiety and an AB spin system of another 8′-substituted coumarin moiety. A singlet at δ 6.11 ascribed to H-3′ and the signal of H-3 disappeared. Apart from the carbon signals of two methyl groups (δ 16.6 and 18.9), there remained 16 aromatic carbons and two lactone carbons at δ 162.9 and 163.9 in the ^{13}C NMR spectrum. Two relatively downfield-shifted signals of quaternary C atoms at δ 114.0 (C-3) and 115.5 (C-8′) also explained that the two coumarin moieties were linked through a bond between C-3 and C-8′. The structure was further confirmed by the heteronuclear multiple-bond correlation (HMBC) experiment, as the correlations between 4-CH_3 and C-8′ as well as between H-6′ and C-3 established the existence of a C-3−C-8′ bond. The ^1H and ^{13}C resonances were assigned by combination of HMBC, heteronuclear single-quantum coherence (HSQC), and rotating frame Overhauser effect spectroscopy (ROESY). In addition, the relative stereochemistry was elucidated by a ROESY experiment in DMSO-d_6. The absence of the cross-peaks from 4-CH_3 to 7′-OH at δ 10.52 and H-6′ illustrated that they were spatially too far away. Subsequently, a variety of calculations also confirmed this inference (see below). On the basis of these findings, the structure of **1** was elucidated as shown in Figure 1 and named 7,7′-dihydroxy-4,4′-dimethyl-3,8′-bicoumarin.

Compound **2** was obtained as a white, amorphous powder. It might be a coumarin dimer with the same molecular formula, $C_{20}H_{14}O_6$, as **1** from its HRESIMS data. IR absorptions at 3442 and 1620 cm^{-1} were indicative of the existence of hydroxyl and

dx.doi.org/10.1021/jf304384b | J. Agric. Food Chem. 2013, 61, 1501−1508

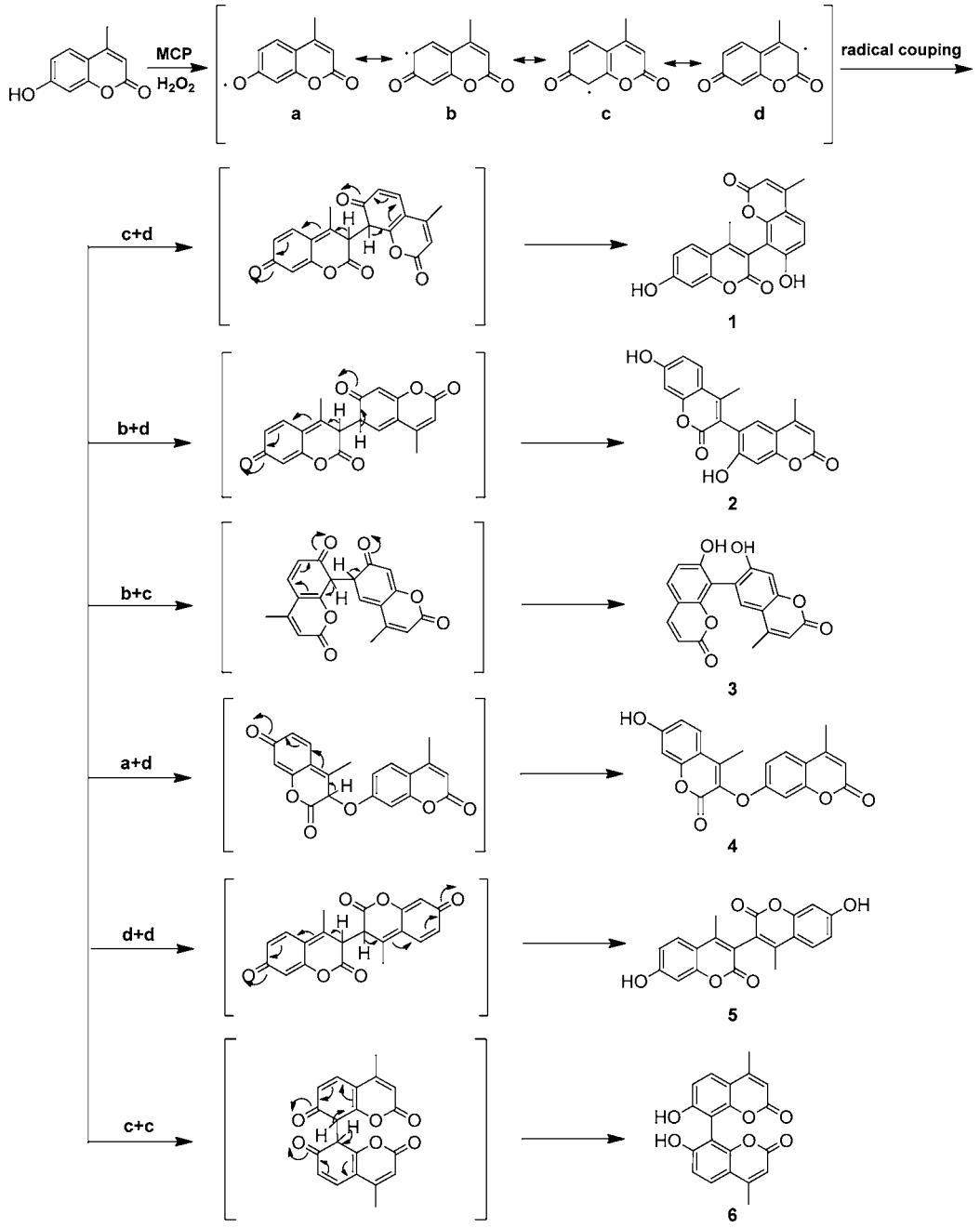

Figure 2. Proposed mechanism for the formation of bicoumarins.

lactone carbonyl groups. In the ^{1}H NMR spectrum, only one olefinic signal at δ 6.08 assignable to characteristic proton H-3′ was observed, which suggested that another olefinic proton, H-3, was replaced. Five aromatic-proton signals were attributed to an ABX system and an AX system, indicating that H-6′ was also replaced. HMBC correlations from H-5′ to C-3 and 4-CH_3 to C-5′ proved the connective position. All the above data suggested that compound **2** was a "C-3−C-6′" bicoumarin. In the ROESY experiment, the nuclear Overhauser effects (NOEs) showed the strong cross signals from H-5 to 4-CH_3, H-5′ to 4′-CH_3, and 4′-CH_3 to H-3′. At the same time, the weak cross signal observed between 4-CH_3 and H-5′ was very critical to verify the stereochemistry. Compound **2** was determined to be 7,7′-dihydroxy-4,4′-dimethyl-3,6′-bicoumarin.

Compound **3** was isolated as a white, amorphous powder and had IR absorption bands at 3424 and 1629 cm^{-1}, suggesting the presence of a hydroxyl function and a carbonyl group. The positive HRESIMS displayed a quasimolecular ion $[M + Na]^+$ at m/z 373.0684, corresponding to the molecular formula $C_{20}H_{14}O_6$, which indicated that the bicoumarin was obtained. The ^{1}H NMR spectrum contained an AB system and an AX system, indicating that H-8 and H-6′ were replaced in the original two coumarin units, respectively. The downfield-shifted resonances for C-8 and C-6′ confirmed the linkage between two coumarin moieties as a C-8−C-6′ bridge. Furthermore, a key HMBC correlation observed from H-5′ to C-8 verified the C-8−C-6′ coupling. Consequently, compound **3** was characterized as 7,7′-dihydroxy-4,4′-dimethyl-8,6′-bicoumarin.

dx.doi.org/10.1021/jf304384b | J. Agric. Food Chem. 2013, 61, 1501−1508

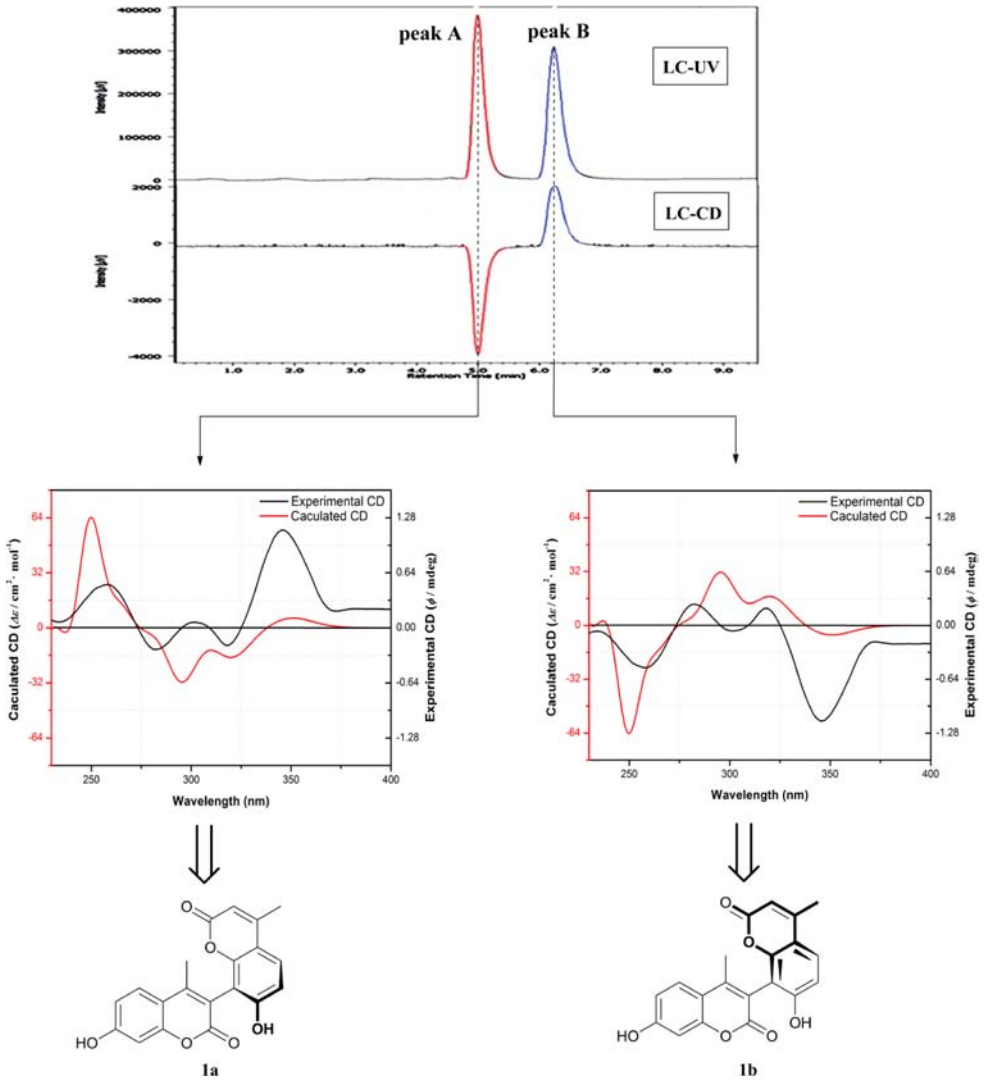

Figure 3. HPLC-UV and HPLC-CD analysis of compound **1** using a chiral phase and assignment of the absolute configurations to **1a** and its atropodiastereomer **1b** by comparison of the experimental CD spectra (stopped-flow mode) with the spectra calculated.

Compound **4** was found to possess a molecular formula of $C_{20}H_{14}O_6$ from its HRESIMS ion at m/z 373.0680 $[M + Na]^+$. Thus, compound **4**, similar to **1**−**3**, also consisted of two 7-hydroxy-4-methylcoumarin units. The IR analysis also indicated the presence of a hydroxyl group (3450 cm^{-1}) and a carbonyl group (1679 cm^{-1}). The ^1H NMR spectrum showed the existence of two ABX spin systems and a single olefinic proton of H-3′, indicating H-3 was substituted. Combined with the molecular weight, compound **4** might be a "C−O−C" dimeric structure. In the ^{13}C NMR spectrum, there was a significant downfield-shifted signal at δ 132.6 (C-3). Correlations of 4-CH_3 (δ 2.29) with C-3 (δ 132.6) and of H-6′ (δ 7.08) and H-8′ (δ 7.05) with C-7′ (δ 160.2) were evident in the HMBC experiment. Furthermore, an NOE correlation between 4-CH_3 and H-6′ also suggested a C-3−O−C-7 ether linkage between the two coumarin units. From the above observations, the structure of **4** was defined as 7-hydroxy-4-methyl-3-(4′-methyl-7′-coumarinyloxy)coumarin.

Additional isolated compounds **5** and **6** were recognized by comparison of their physical and spectroscopic data with those reported in the literature.[31] They were obtained for the first time by direct biotransformation.

Compounds **1**, **2**, **3**, **5**, and **6** were biphenyls and were chiral because of restricted rotation about the single bond connecting the two coumarin units. Nevertheless, these dimers generated from radical reaction should be racemates, consistent with the zero values of optical rotations and a flat line of the CD spectra. On the basis of the aim to characterize these compounds, compound **1** was taken for example to study the stereochemical assignments.

Online HPLC-CD analysis was carried out to examine the absolute configuration of **1** on a chiral column. A couple of enantiomers were well separated and equivalent, with a negative LC-CD signal for the faster eluting peak (peak A) and a positive signal for the slower peak (peak B). Meanwhile, the flow was stopped at the maxima of the CD signals to obtain the CD spectra (Figure 3). To further corroborate the absolute configuration, we applied the methodology of time-dependent density functional theory (TDDFT) to calculate the ECD spectra of **1**. The geometries were optimized first and then calculated at the B3LYP/6-31G+(d,p) level using the TDDFT method. The results were compared with experimental CD data. The spectrum computed for *P* configuration was in very good agreement with the CD curve measured for peak A, whereas the spectrum calculated for *M* configuration matched

dx.doi.org/10.1021/jf304384b | J. Agric. Food Chem. 2013, 61, 1501−1508

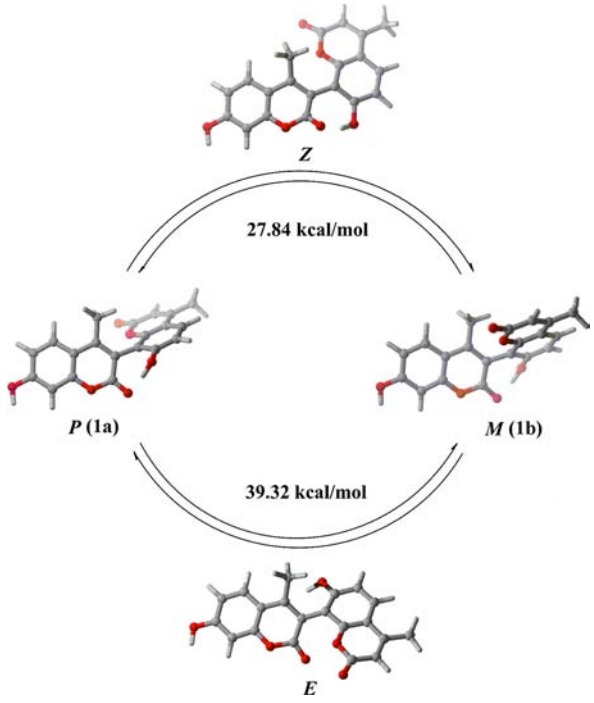

Figure 4. Optimized structures for the ground state and *E*- and *Z*-transition states of compound **1**. For **1a** and **1b**, dark gray fragments are out-of-plane. Rotational energy barriers (in kcal/mol) are also shown.

Table 2. Inhibitory Activities on Yeast α-Glucosidase[a]

compound	inhibition ratio (%)[b]	IC_{50} (μM)
1	66.25 ± 0.70	36.80 ± 0.35
2	69.60 ± 0.35	16.30 ± 0.22
3	32.82 ± 3.27	271.76 ± 1.87
4	21.13 ± 7.38	555.73 ± 4.31
5	13.58 ± 4.11	294.46 ± 2.06
6	13.52 ± 8.18	>600
7-OH-4-CH_3 coumarin	17.96 ± 7.67	558.09 ± 4.52
1-deoxynojirimycin	55.26 ± 0.98	107.21 ± 0.66
genistein	52.65 ± 0.62	36.02 ± 0.33

[a]All compounds were examined in a set of experiments repeated three times independently. [b]Percent inhibition at a concentration of 100 μM.

well with peak B (Figure 3). Thus, the absolute configuration of **1a** was the *P* configuration, and that of **1b** was the *M* configuration.

The dihedral angle scan between the two coumarin rings of **1a** and **1b** was investigated using DFT methods at the 6-31G +(d,p) level, as depicted in Figure 4. Only one minimum-energy conformation, in accord with the NMR experiments, was found for the nonplanar ground state of **1**. According to the DFT data, the dihedral angles in the minimum structure of **1** were 125.8° for the *P* configuration and −126.2° for the *M* configuration. Additionally, the calculations revealed that there were two transition states to make the interconversion of the pair of enantiomers **1a** and **1b**. One enantiomer was from the *E*-transition state with the rotational energy barrier of 39.32 kcal/mol, whereas the other was via the *Z*-transition state with barrier of 27.84 kcal/mol. The rotational energy barriers arose from the steric bulk of substituents in the *o*-positions, which were sufficiently high to prevent the interconversion of the two

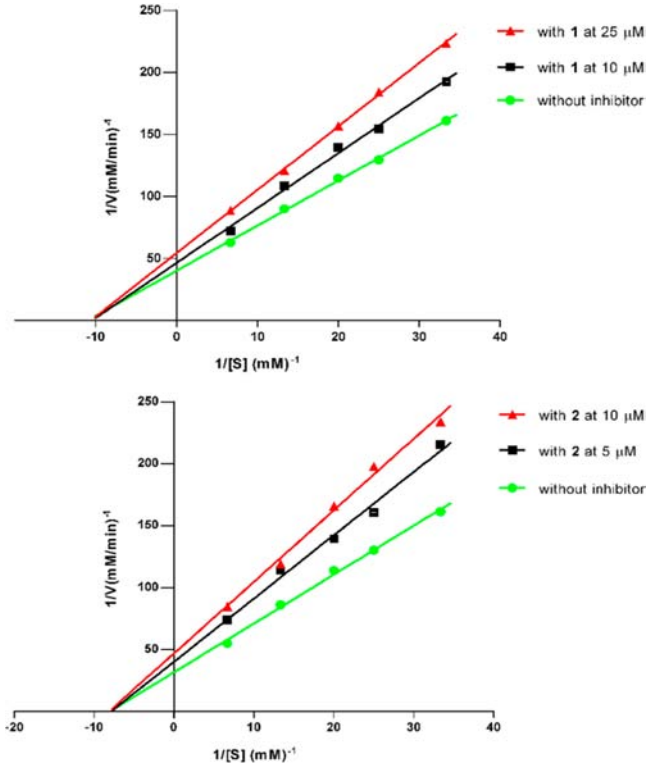

Figure 5. Double-reciprocal plots of the inhibition kinetics of α-glucosidase by compounds **1** and **2**. α-Glucosidase was treated with various concentrations of *p*-NPG in the absence or presence of inhibitors at two different concentrations.

Table 3. Effects of 1 and 2 on the Secondary Structure of α-Glucosidase

compound	α-helix (%)	β-sheet (%)	β-turn (%)	random (%)
without inhibitor	29.2	29.9	9.8	31.1
1 (50 μm)	24.5	34.3	11.3	29.9
1 (100 μm)	24.0	32.6	10.1	33.2
without inhibitor	28.4	36.4	3.2	32.0
2 (30 μm)	26.1	44.0	2.2	27.7
2 (60 μm)	21.6	51.7	0.7	26.0

enantiomers at room temperature. As a result, the two enantiomers **1a** and **1b** could coexist stably at room temperature, which also illustrated that it was the radical reaction that contributed to the racemization of the biotransformation products.

α-Glucosidase Inhibitory Activity. The enzyme inhibition activity for yeast α-glucosidase was assessed using *p*-NPG as a substrate and 1-deoxynojirimycin[8] and genistein[32] as positive controls. These compounds were used in dose-dependent experiments (data not shown), indicating that **1** and **2** of the tested compounds had high binding affinity toward α-glucosidase. In this *in vitro* activity test, compounds **1** and **2** exhibited significant inhibitory activities against α-glucosidase, more than 1-deoxynojirimycin (107.21 μM), while 7-hydroxy-4-methylcoumarin, the substrate of the enzymatic reaction by MCP, exhibited weak activity (Table 2). In particular, compound **2** exhibited stronger inhibitory activity, with an IC_{50} value of 16.30 μM, being more effective than genistein (36.02 μM).

Kinetics of the representative α-glucosidase inhibitors was further studied to determine the type of inhibition by the

dx.doi.org/10.1021/jf304384b | J. Agric. Food Chem. 2013, 61, 1501−1508

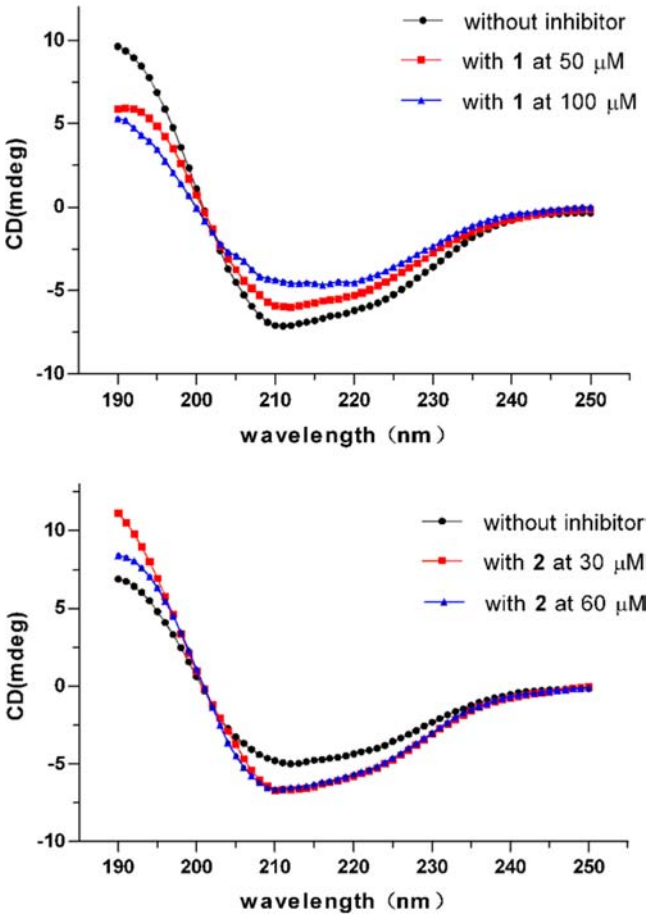

Figure 6. Circular dichroism spectra of α-glucosidase after enzyme interactions with compounds **1** and **2**.

analysis of the Lineweave−Burk plots, as depicted in Figure 5. In addition, double-reciprocal plots showed that increasing the concentration of inhibitors produced a set of lines with a common intercept on the *x*-axis but with different gradients. These data were consistent with a noncompetitive inhibition; the K_i values for **1** and **2** were 63.45 and 19.12 μM, respectively. Hence, the inhibitors were expected to bind to a site other than the active site of α-glucosidase.

A series of conformational changes of the enzyme evoked by an inhibitor were an indispensable part of the action mechanism and regulation of biological activity.[33,34] Circular dichroism spectroscopy provided an experimentally very convenient and reasonably fast method of identifying such changes examined in characteristic spectral regions. Thus, CD was applied to observe the secondary structure of α-glucosidase in complex with inhibitors. Analysis of the total secondary structure content gave values of α-helix, β-sheet, β-turn, and random contents, as estimated by the method of Greenfield.[35] As shown in Table 3, the inhibitors triggered slight changes of α-glucosidase, by decreasing the α-helix (from 29.2% to 24.0% and 28.4% to 21.6% for **1** and **2**, respectively) and increasing the β-sheet content (from 29.9% to 32.6% and 36.4% to 51.7% for **1** and **2**, respectively) in a dose-dependent manner. These findings further supported the proposition that the inhibitors rearranged its secondary structure and influenced the folding organization of α-glucosidase (Figure 6). Hence, it might be part of the mechanism of the enzymatic inhibition required to prevent the hydration of the substrate binding site and also required to induce the cleft closure to avoid entrance of the substrate.[36]

In conclusion, this study was the first example to biosynthesize bicoumarins by a peroxidase-active, pure preparation from *M. charantia* as a new substitute source of an oxidative enzyme that could have extensive biocatalytic applications. Moreover, this pathway was well-recognized as a "green" process and ruled out tedious multistep reactions and toxic byproducts common in organic reactions. The bioactivity analysis demonstrated that compounds **1** and **2** revealed significant inhibitory effects on yeast α-glucosidase, with IC_{50} values at low micromolar concentrations. Therefore, this type of bicoumarin may provide a useful template to help future development in the search for new hypoglycemic agents.

■ ASSOCIATED CONTENT

Supporting Information

HPLC chromatogram of the experimental controls and the biotransformation reaction. This material is available free of charge via the Internet at http://pubs.acs.org.

■ AUTHOR INFORMATION

Corresponding Author

*Tel/Fax: +86-25-83271405. E-mail: cpu_lykong@126.com.

Funding

This research work was supported by the Program for Changjiang Scholars and Innovative Research Team in University (PCSIRTIRT1193), the Project Founded by the Priority Academic Program Development of Jiangsu Higher Education Institutions (PAPD), the Cultivation Fund of the Key Scientific and Technical Innovation Project, Ministry of Education of China (No. 707033), and the Scaling Project for Innovation Scholars, Natural Science Foundation of Jiangsu Province, China (BK2008039).

Notes

The authors declare no competing financial interest.

■ REFERENCES

(1) Lim, E. L.; Hollingsworth, K. G.; Aribisala, B. S.; Chen, M. J.; Mathers, J. C.; Taylor, R. Reversal of type 2 diabetes: normalisation of beta cell function in association with decreased pancreas and liver triacylglycerol. *Diabetologia* **2011**, *54*, 2506−2514.

(2) Choo, C. Y.; Sulong, N. Y.; Man, F.; Wong, T. W. Vitexin and isovitexin from the leaves of *Ficus deltoidea* with *in-vivo* α-glucosidase inhibition. *J. Ethnopharmacol.* **2012**, *142*, 776−781.

(3) Agardh, E.; Allebeck, P.; Hallqvist, J.; Moradi, T.; Sidorchuk, A. Type 2 diabetes incidence and socio-economic position: a systematic review and meta-analysis. *Int. J. Epidemiol.* **2011**, *40*, 804−818.

(4) Yokozawa, T.; Kim, H. Y.; Cho, E. J. Erythritol attenuates the diabetic oxidative stress through modulating glucose metabolism and lipid peroxidation in streptozotocin-induced diabetic rats. *J. Agric. Food Chem.* **2002**, *50*, 5485−5489.

(5) Ou, S. Y.; Kwok, K. C.; Li, Y.; Fu, L. In vitro study of possible role of dietary fiber in lowering postprandial serum glucose. *J. Agric. Food Chem.* **2001**, *49*, 1026−1029.

(6) Maki, K. C. Dietary factors in the prevention of diabetes mellitus and coronary artery disease associated with the metabolic syndrome. *Am. J. Cardiol.* **2004**, *93*, 12−17.

(7) Seo, W. D.; Kim, J. H.; Kang, J. E.; Ryu, H. W.; Curtis-Long, M. J.; Lee, H. S.; Yang, M. S.; Park, K. H. Sulfonamide chalcone as a new class of α-glucosidase inhibitors. *Bioorg. Med. Chem. Lett.* **2005**, *15*, 5514−5516.

(8) Kwon, H. J.; Chung, J. Y.; Kim, J. Y.; Kwon, O. Comparison of 1-deoxynojirimycin and aqueous mulberry leaf extract with emphasis on

postprandial hypoglycemic effects: in vivo and in vitro studies. *J. Agric. Food Chem.* **2011**, *59*, 3014−3019.
(9) Cumpstey, I.; Ramstadius, C.; Eszter Borbas, K.; Alonzi, D. S.; Butters, T. D. Synthesis and α-glucosidase II inhibitory activity of valienamine pseudodisaccharides relevant to *N*-glycan biosynthesis. *Bioorg. Med. Chem. Lett.* **2011**, *21*, 5219−5223.
(10) Yee, H. S.; Fong, N. T. A review of the safety and efficacy of acarbose in diabetes mellitus. *Pharmacotherapy* **1996**, *16*, 792−805.
(11) Alcalde, M.; Ferrer, M.; Plou, F. J.; Ballesteros, A. Environmental biocatalysis: from remediation with enzymes to novel green processes. *Trends Biotechnol.* **2006**, *24*, 281−287.
(12) Wohlgemuth, R. Biocatalysis—key to sustainable industrial chemistry. *Curr. Opin. Biotechnol.* **2010**, *21*, 713−724.
(13) Liu, X.; Xie, D.; Chen, R.; Mei, M.; Zou, J. H.; Chen, X. G.; Dai, J. G. A furantaxane with an unusual 6/8/6/5 ring system and potent tumor MDR reversal activity obtained via microbial transformation. *Org. Lett.* **2012**, *14*, 4106−4109.
(14) Ning, L. L.; Zhan, J. X.; Qu, G. Q.; Zhong, L.; Guo, H. Z.; Bi, K. S.; Guo, D. A. Biotransformation of triptolide by *Cunninghamella blakesleana*. *Tetrahedron* **2003**, *59*, 4209−4213.
(15) Bunzel, M.; Heuermann, B.; Kim, H.; Ralph, J. Peroxidase-catalyzed oligomerization of ferulic acid esters. *J. Agric. Food Chem.* **2008**, *56*, 10368−10375.
(16) Wilkens, A.; Paulsen, J.; Wray, V.; Winterhalter, P. Structures of two novel trimeric stilbenes obtained by horseradish peroxidase catalyzed biotransformation of trans-resveratrol and (−)-ε-viniferin. *J. Agric. Food Chem.* **2010**, *58*, 6754−6761.
(17) Takaya, Y.; Yan, K.-X.; Terashima, K.; He, Y.-H.; Niwa, M. Biogenetic reactions on stilbenetetramers from Vitaceaeous plants. *Tetrahedron* **2002**, *58*, 9265−9271.
(18) Ou, L.; Kong, L. Y.; Zhang, X. M.; Niwa, M. Oxidation of ferulic acid by *Momordica charantia* peroxidase and related anti-inflammation activity changes. *Biol. Pharm. Bull.* **2003**, *26*, 1511−1516.
(19) Liu, H. L.; Wan, X.; Huang, X. F.; Kong, L. Y. Biotransformation of sinapic acid catalyzed by *Momordica charantia* peroxidase. *J. Agric. Food Chem.* **2007**, *55*, 1003−1008.
(20) Yu, B. B.; Han, X. Z.; Lou, H. X. Oligomers of resveratrol and ferulic acid prepared by peroxidase-catalyzed oxidation and their protective effects on cardiac injury. *J. Agric. Food Chem.* **2007**, *55*, 7753−7757.
(21) Wan, X.; Wang, X. B.; Yang, M. H.; Wang, J. S.; Kong, L. Y. Dimerization of piceatannol by Momordica charantia peroxidase and α-glucosidase inhibitory activity of the biotransformation products. *Bioorg. Med. Chem.* **2011**, *19*, 5085−5092.
(22) Kempen, I.; Papapostolou, D.; Thierry, N.; Pochet, L.; Counerotte, S.; Masereel, B.; Foidart, J. M.; Reboud-Ravaux, M. J.; Noel, A.; Pirotte, B. 3-Bromophenyl 6-acetoxymethyl-2-oxo-2*H*-1-benzopyran-3-carboxylate inhibits cancer cell invasion *in vitro* and tumour growth *in vivo*. *Br. J. Cancer* **2003**, *88*, 1111−1118.
(23) Céspedes, C. L.; Avila, J. G.; Martínez, A.; Serrato, B.; Calderón-Mugica, J. C.; Salgado-Garciglia, R. Antifungal and antibacterial activities of Mexican Tarragon (*Tagetes lucida*). *J. Agric. Food Chem.* **2006**, *54*, 3521−3527.
(24) Yu, D.; Suzuki, M.; Xie, L.; Morris-Natschke, S. L.; Lee, K. H. Recent progress in the development of coumarin derivatives as potent anti-HIV agents. *Med. Res. Rev.* **2003**, *23*, 322−345.
(25) Murakami, A.; Gao, G.; Kim, O. K.; Omura, M.; Yano, M.; Ito, C.; Furukawa, H.; Jiwajinda, S.; Koshimizu, K.; Ohigashi, H. Identification of coumarins from the fruit of *Citrus hystrix* DC as inhibitors of nitric oxide generation in mouse macrophage RAW 264.7 cells. *J. Agric. Food Chem.* **1999**, *47*, 333−339.
(26) Raju, B. C.; Tiwari, A. K.; Kumar, J. A.; Ali, A. Z.; Agawane, S. B.; Saidachary, G.; Madhusudana, K. α-Glucosidase inhibitory antihyperglycemic activity of substituted chromenone derivatives. *Bioorg. Med. Chem.* **2010**, *18*, 358−365.
(27) Shen, Q.; Shao, J. L.; Peng, Q.; Zhang, W. J.; Ma, L.; Chan, A. S. C.; Gu, L. Q. Hydroxycoumarin derivatives: novel and potent α-glucosidase inhibitors. *J. Med. Chem.* **2010**, *53*, 8252−8259.
(28) Frisch, M. J; Trucks, G. W.; Schlegel, H. B.; Scuseria, G. E.; Robb, M. A.; Cheeseman, J. R.; Scalmani, G.; Barone, V.; Mennucci, B.; Petersson, G. A.; Nakatsuji, H.; Caricato, M.; Li, X.; Hratchian, H. P.; Izmaylov, A. F.; Bloino, J.; Zheng, G.; Sonnenberg, J. L.; Hada, M.; Ehara, M.; Toyota, K.; Fukuda, R.; Hasegawa, J.; Ishida, M.; Nakajima, T.; Honda, Y.; Kitao, O.; Nakai, H.; Vreven, T.; Montgomery, J. A., Jr.; Peralta, J. E.; Ogliaro, F.; Bearpark, M.; Heyd, J. J.; Brothers, E.; Kudin, K. N.; Staroverov, V. N.; Keith, T.; Kobayashi, R.; Normand, J.; Raghavachari, K.; Rendell, A.; Burant, J. C.; Iyengar, S. S.; Tomasi, J.; Cossi, M.; Rega, N.; Millam, J. M.; Klene, M.; Knox, J. E.; Cross, J. B.; Bakken, V.; Adamo, C.; Jaramillo, J.; Gomperts, R.; Stratmann, R. E.; Yazyev, O.; Austin, A. J.; Cammi, R.; Pomelli, C.; Ochterski, J. W.; Martin, R. L.; Morokuma, K.; Zakrzewski, V. G.; Voth, G. A.; Salvador, P.; Dannenberg, J. J.; Dapprich, S.; Daniels, A. D.; Farkas, O.; Foresman, J. B.; Ortiz, J. V.; Cioslowski, J.; and Fox, D. J. *Gaussian 09*, Revision B.01; Gaussian, Inc.: Wallingford, CT, 2010.
(29) Stephens, P. J.; Harada, N. ECD Cotton effect approximated by the Gaussian curve and other methods. *Chirality* **2010**, *22*, 229−233.
(30) Tsujii, E.; Muroi, M.; Shiragami, N.; Takatsuki, A. Nectrisine is a potent inhibitor of alpha-glucosidases, demonstrating activities similarly at enzyme and cellular levels. *Biochem. Biophys. Res. Commun.* **1996**, *220*, 459−466.
(31) Lele, S. S.; Patel, M. G.; Sethna, S. Synthesis of some bicoumarinyl and 8-phenylcoumarin derivatives. *J. Chem. Soc.* **1961**, 969−971.
(32) Lee, D. S.; Lee, S. H. Genistein, a soy isoflavone, is a potent alpha-glucosidase inhibitor. *FEBS Lett.* **2001**, *501*, 84−86.
(33) Kelly, S. M.; Jess, T. J.; Price, N. C. How to study proteins by circular dichroism. *Biochim. Biophys. Acta* **2005**, *1751*, 119−139.
(34) Greenfield, N. J. Methods to estimate the conformation of proteins and polypeptides from circular dichroism data. *Anal. Biochem.* **1996**, *235*, 1−10.
(35) Greenfield, N.; Davidson, B.; Fasman, G. D. The use of computed optical rotatory dispersion curves for the evaluation of protein conformation. *Biochemistry* **1967**, *6*, 1630−1637.
(36) Marques, M. R.; Vaso, A.; Neto, J. R.; Fossey, M. A.; Oliveira, J. S.; Basso, L. A.; dos Santos, D. S.; de Azevedo, W. F., Jr.; Palma, M. S. Dynamics of glyphosate-induced conformational changes of *Mycobacterium tuberculosis* 5-enolpyruvylshikimate-3-phosphate synthase (EC 2.5.1.19) determined by hydrogen-deuterium exchange and electrospray mass spectrometry. *Biochemistry* **2008**, *47*, 7509−7522.